Pattern formation in parametric sound generation

Isabel Pérez-Arjona and Víctor J. Sánchez-Morcillo
Departament de Física Aplicada, Universitat Politécnica de València, Crta. Natzaret-Oliva s/n, 46730 Grau de Gandia, Spain
(Received 25 April 2005; published 1 December 2005)

Pattern formation of sound is predicted in a driven resonator where subharmonic generation takes place. A model allowing for diffraction of the fields (large-aspect-ratio limit) is derived by means of the multiple-scale expansion technique. An analysis of the solutions and its stability against space-dependent perturbations is performed in detail considering the distinctive peculiarities of the acoustical system. Numerical integration confirms the analytical predictions and shows the possibility of patterns in the form of stripes and squares.

DOI: 10.1103/PhysRevE.72.066202 PACS number(s): 43.25.+y, 89.75.Kd

I. INTRODUCTION

The topic of pattern formation, or the spontaneous emergence of ordered structures, is nowadays an active field of research in many areas of nonlinear science [1]. Transverse modes may become unstable when the amplitude of the external input reaches a critical threshold value, large enough to overcome the losses produced by dissipative processes in the system, and a symmetry breaking transition can develop, carrying the system from an initially homogeneous to an inhomogeneous state, usually with spatial periodicity. Pattern formation is commonly observed in large-aspect-ratio nonlinear systems (either physical, biological, chemical, etc.) which are driven far from the equilibrium state by an external input [1].

Parametrically driven systems offer many examples of spontaneous pattern formation. For example, parametric excitation of surface waves by a vertical shake (Faraday instability) in fluids [2] and granular layers [3], spin waves in ferrites and ferromagnets, and Langmuir waves in plasmas parametrically driven by a microwave field [4] or the optical parametric oscillator [5,6] have been studied. In nonlinear acoustics, a phenomenon which belongs to the class of the previous examples is parametric sound amplification. As will be shown later, when large-aspect-ratio nonlinear acoustic resonators are considered, dissipative structures can also emerge spontaneously, which allows one to incorporate nonlinear acoustics into the broad field of pattern formation in nonlinear sciences.

Parametric sound amplification consists of the resonant interaction of a triad of sound waves with frequencies ω_0, ω_1, and ω_2, for which the following energy and momentum conservation conditions are fulfilled:

$$\omega_0 = \omega_1 + \omega_2,$$

$$\vec{k}_0 = \vec{k}_1 + \vec{k}_2 + \Delta\vec{k}, \tag{1}$$

where $\Delta\vec{k}$ is a small phase mismatch. The process is initiated by an input pumping wave of frequency ω_0 which, due to the coupling to the nonlinear medium, generates a pair of waves with frequencies ω_1 and ω_2. When the wave interaction occurs in a resonator, a threshold value for the input amplitude is required, and the process is called parametric sound generation. In acoustics, this process has been described by several authors under different conditions, either theoretical and experimentally: In [7–9] the one-dimensional case (collinearly propagating waves) is considered, and in [10] the problem of interaction between concrete resonator modes, with a given transverse structure, is studied. In both cases, small-aspect-ratio resonators, containing liquid and gas, respectively, are considered. More recently, the parametric interaction in a large-aspect-ratio resonator filled with superfluid ^{4}He has been investigated [11].

It is well known that optical and acoustical waves share many common phenomena, an analogy which sometimes can be extended to the nonlinear regime [12]. In particular, the phenomenon of parametric sound generation is analogous to optical parametric oscillation in nonlinear optics. However, an important difference between acoustics and optics is the absence of dispersion in the former. In a nondispersive medium, all the harmonics of each initial monochromatic wave propagate synchronously. As a consequence, the spectrum broadens during propagation and the energy is continuously pumped into the higher harmonics, leading to wave-form distortion and eventually to the formation of shock fronts. On the contrary, dispersion allows that only few modes, those satisfying given synchronism conditions, participate effectively in the interaction process.

In acoustics, the presence of higher harmonics can be avoided by different means. One method is based on the introduction of some dispersion mechanism. In finite geometries, such as waveguides [13] or resonators [14], the dispersion is introduced by the lateral boundaries. Different resonance modes, propagating at different angles, propagate with different effective phase velocities. Other proposed methods are, for example, the inclusion of media with selective absorption, in which selected spectral components undergo strong losses and may be removed from the wave field [16], or resonators where the end walls present a frequency-dependent complex impedance [9]. In this case, the resonance modes of the resonator are not integrally related, and by proper adjustment of the resonator parameters one can get that only few modes, those lying close enough to a cavity resonance, reach a significant amplitude. In any of these cases, a spectral approach to the problem, in terms of few interacting modes, is justified.

Therefore the selective effect of the resonator allows one to reduce the study of parametric sound generation to the interaction of three field modes, corresponding to the driving

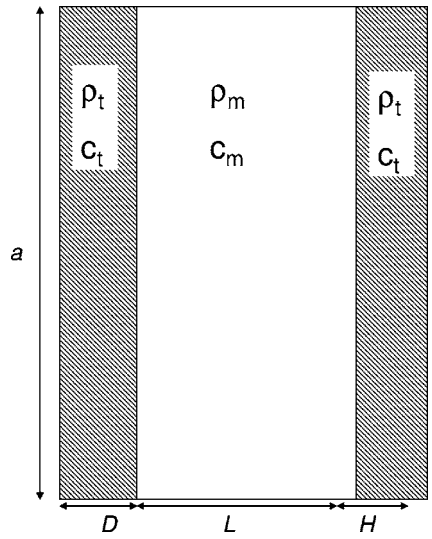

FIG. 1. Scheme of a three-element acoustic resonator. Each section is acoustically characterized by its density an propagation velocity of sound.

(fundamental) and subharmonic frequencies, and to describe this interaction through a small set of nonlinear coupled differential equations. In the present work we concentrate on the particular degenerate case of subharmonic generation, where $\omega_1=\omega_2$ and consequently $\omega_0=2\omega_1$, ω_0 being the fundamental and ω_1 the generated subharmonic, both quasiresonant with a corresponding resonance mode. This degenerate case has been considered in previous experimental studies [9,14] in the case of small-aspect-ratio cavities where transverse spatial evolution is absent.

The aim of the paper is twofold: to provide a rigorous derivation of the dynamical model describing the parametric interaction of acoustic waves in a large-aspect-ratio cavity, as this derivation does not exist to the best of our knowledge, and to determine the conditions under which pattern formation of sound could be observed in an acoustic system. Interestingly, the derived model, obtained from the basic hydrodynamics equations, turns out to be isomorphous to the system of equations describing parametric oscillation in an optical resonator. Such isomorphism is a very encouraging result: On the one hand, solutions similar to those known for optical parametric oscillation can be expected to occur in parametric sound generation and on the other hand, this result firmly links pattern formation in cavity nonlinear acoustics with the wider field of pattern formation in nonlinear science. Numerical integrations under realistic acoustical parameters confirm the predicted results.

II. DERIVATION OF THE MODEL

A. Three-wave interaction in an acoustic resonator

The physical system we consider in this paper is an acoustic cavity (resonator) composed of two parallel solid walls, with thicknesses D and H located at a distance L, containing a fluid medium inside, as described in Fig. 1. The different media are acoustically characterized by their density ρ and the propagation velocity of the sound wave, c. One of the walls vibrates at a frequency close to one of the normal modes of the cavity.

The resonance modes f (eigenfrequencies) of such resonator can be calculated by using the equation [9]

$$\mathcal{R}\left(\tan\frac{f}{f_D}\pi+\tan\frac{f}{f_H}\pi\right)+\left(1-\mathcal{R}^2\tan\frac{f}{f_D}\pi\tan\frac{f}{f_H}\pi\right)\tan\frac{f}{f_L}\pi=0, \quad (2)$$

where $\mathcal{R}=\rho_w c_w/\rho c$ is the ratio of wall to medium acoustic impedances, and $f_D=c_w/2D$, $f_H=c_w/2H$, and $f_L=c/2L$ are the fundamental resonance frequencies of each individual region, respectively. From the numerical solutions of Eq. (2) results a nonequidistant spectrum, the position of the different modes being determined by the properties and dimensions of the different elements. Note that the particular case corresponding to an equidistant spectrum (constant free spectral range) is obtained as a limit case when we impose infinite reflectance at the walls ($\mathcal{R}\to\infty$) with negligible thickness. In this case Eq. (2) reduces to $\tan kL=0$ and the modes obey the Fabry-Perot condition $k=n\pi/L$. In such a perfect resonator, any harmonic of a resonant driving wave is also resonant with a higher-order cavity mode and the energy flow into these modes leads to wave distortion and invalidates a modal description of the problem in terms of the interaction among few waves.

In a lossy resonator, however, one can get the second harmonic of the driving wave to be more detuned than subharmonics with respect to a cavity resonance, thus reducing the effectivity of the cascade process into the higher harmonics. This effect is enhanced in the case of viscous media, in which the higher frequencies experience stronger losses (absorption). Furthermore, it is possible to get subharmonic generation slightly detuned from a cavity resonance, which is a necessary condition for the development of spatial instabilities, as will be discussed in the following sections. These two facts justify the description of high-intensity acoustic waves in a resonator in terms of the interaction among few frequency components. Several experimental results demonstrate this fact [7–9] and support the validity of this assumption in the theoretical approach.

The main novelty of this work with respect to previous studies is to consider the diffraction of the waves inside the cavity. Diffraction can play an important role when the cavity has a large Fresnel number, defined as $F=a^2/\lambda L$, where a is the characteristic transverse size of the cavity (for example, a^2 is the area of a plane radiator), λ is the wavelength, and L is the length of the cavity in the direction of propagation, considered the longitudinal axis of the cavity. Sometimes the case of large F is called the large-aspect-ratio limit. All these assumptions will be taken into account in the derivation of the model in the next section.

B. Hydrodynamic equations for sound waves

As a starting point of the analysis, we consider the basic hydrodynamic equations describing the propagation of sound waves in liquids and gases—namely, the continuity (mass conservation) equation

$$\frac{\partial \rho}{\partial t} + \boldsymbol{\nabla}(\rho \mathbf{u}) = 0 \tag{3}$$

and the Euler (momentum conservation) equation

$$\rho\left(\frac{\partial}{\partial t} + \mathbf{u}\,\boldsymbol{\nabla}\right)\mathbf{u} = -\boldsymbol{\nabla} p + \mu \nabla^2 \mathbf{u} + \left(\mu_B + \frac{\mu}{3}\right)\boldsymbol{\nabla}(\boldsymbol{\nabla}\mathbf{u}), \tag{4}$$

where ρ is the density of the medium, $\mathbf{u}$ is the fluid particle velocity, p is the thermodinamic pressure, and μ and μ_B represent shear and bulk viscosities, respectively. Equations (3) and (4) must be complemented by the equation of state $p=p(\rho)$. If the losses due to viscosity are small (due just to heat conduction), the process can be assumed to be adiabatic. Then the pressure in the state equation can be expanded around the equilibrium and the equation of state takes the form

$$\begin{aligned} p &= p_0 + \left(\frac{\partial p}{\partial \rho}\right)_s \rho' + \frac{1}{2}\left(\frac{\partial^2 p}{\partial \rho^2}\right)_s^2 \rho'^2 + \cdots \\ &= p_0 + c_0^2 \rho' + \frac{1}{2}\Gamma \rho'^2 + \cdots, \end{aligned} \tag{5}$$

where $\rho' = \rho - \rho_0$, ρ_0 being the equilibrium value of the density, $c_0 = \sqrt{(\partial p/\partial \rho)_s}$ is the (low-amplitude) sound velocity, and

$$\Gamma = \left(\frac{\partial^2 p}{\partial \rho^2}\right)_s = \frac{c_0^2}{\rho_0}\frac{B}{A},$$

where B/A is commonly used in acoustics as the nonlinearity parameter and has been measured in different media [15]. The subscript s denotes the adiabatic character of the process and the ellipsis in Eq. (5) the nonlinearities higher than quadratic, which are neglected.

Substitution of Eq. (5) in Eq. (4) leads to

$$\begin{aligned} \rho\left(\frac{\partial}{\partial t} + \mathbf{u}\,\boldsymbol{\nabla}\right)\mathbf{u} = &- c_0^2 \boldsymbol{\nabla}\rho' - \frac{1}{2}\Gamma \boldsymbol{\nabla}\rho'^2 + \mu \nabla^2 \mathbf{u} \\ &+ \left(\mu_B + \frac{\mu}{3}\right)\boldsymbol{\nabla}(\boldsymbol{\nabla}\mathbf{u}), \end{aligned} \tag{6}$$

which together with Eq. (3) is a two-variable model. It is convenient to write Eqs. (3) and (6) in nondimensional form, adopting the following normalizations:

$$\mathbf{v} \equiv \frac{\mathbf{u}}{V}, \quad \bar{\rho} \equiv \frac{\rho}{\rho_0}, \tag{7}$$

where V is a reference velocity, small compared with c_0. Also, time and space are defined as

$$\bar{t} = \omega t, \quad \bar{\mathbf{x}} = k\mathbf{x}. \tag{8}$$

where ω and k are the angular frequency and wave number of a reference wave and obey $\omega = kc_0$. With this normalization Eqs. (3) and (6) have the form

$$\frac{\partial \bar{\rho}}{\partial \bar{t}} + M\rho \bar{\boldsymbol{\nabla}}\mathbf{v} + M\mathbf{v}\bar{\boldsymbol{\nabla}}\bar{\rho} = 0, \tag{9}$$

$$M\bar{\rho}\frac{\partial \mathbf{v}}{\partial \bar{t}} + M^2 \bar{\rho}\mathbf{v}\bar{\boldsymbol{\nabla}}\mathbf{v} = -\bar{\boldsymbol{\nabla}}\bar{\rho} - \frac{1}{2}\bar{\Gamma}\bar{\boldsymbol{\nabla}}(\bar{\rho}-1)^2 + \bar{\mu}M^2\bar{\nabla}^2\mathbf{v}, \tag{10}$$

where the losses $\bar{\mu}$, the nonlinearity $\bar{\Gamma}$, and the acoustic Mach number M are parameters defined as

$$\bar{\mu} = \frac{k}{\rho_0 V}\left(\mu_B + \frac{4}{3}\mu\right), \tag{11}$$

$$\bar{\Gamma} = \frac{\rho_0}{c_0^2}\Gamma \equiv \frac{B}{A}, \tag{12}$$

$$M = \frac{V}{c_0}. \tag{13}$$

In Eq. (10) we have used the identity $\boldsymbol{\nabla}(\boldsymbol{\nabla}\mathbf{v}) = \nabla^2\mathbf{v} + \boldsymbol{\nabla} \times \boldsymbol{\nabla} \times \mathbf{v}$, where the second (vorticity) term has been neglected, since its magnitude decays exponentially away from the boundaries [15].

C. Perturbative expansion in the small-Mach-number limit

Under usual conditions, the acoustic Mach number takes small values ($M < 10^{-3}$), which allows us to treat Eqs. (3) and (6) by perturbative techniques. Thus we consider a smallness parameter ε as the Mach number and express the parameters and variables in terms of it.

Let us assume that in the dispersive resonator the changes of the shape of the wave as a consequence of dissipation and nonlinearity, both along the direction of propagation and transverse to it, are small. Also, we take into account that the changes along the transverse direction to the propagation, due to diffraction, take place faster than along this propagation direction [17]. These assumptions allow us to consider the problem in terms of fast and slow scales. A choice of scales accounting for these changes is

$$\bar{t} = T + \varepsilon \tau, \tag{14a}$$

$$(\bar{z}, \bar{x}, \bar{y}) = (z, \sqrt{\varepsilon}x, \sqrt{\varepsilon}y), \tag{14b}$$

and expand the state variables $\bar{\rho}$ and $\mathbf{v} = (v_x, v_y, v_z)$ as

$$\bar{\rho} = 1 + \varepsilon\rho_1 + \varepsilon^2\rho_2, \tag{15a}$$

$$v_z = v_{1z} + \varepsilon v_{2z}, \tag{15b}$$

$$v_x = \sqrt{\varepsilon}v_{1x} + \varepsilon\sqrt{\varepsilon}v_{2x}, \tag{15c}$$

$$v_y = \sqrt{\varepsilon}v_{1y} + \varepsilon\sqrt{\varepsilon}v_{2y}. \tag{15d}$$

where the order of the transverse components of the velocity is determined by the (slow) divergence of the beam [17]. Note that, since at equilibrium fluid is at rest and, on other hand, v is nondimensionalized by V (a reference velocity smaller than c_0), the variation of v is order $O(1)$. Substituting these expressions into Eqs. (9) and (10), we obtain equations

at different orders which can be recursively solved. The leading order $O(\varepsilon)$ reads

$$\frac{\partial v_{1z}}{\partial T} = -\frac{\partial \rho_1}{\partial z}, \tag{16a}$$

$$\frac{\partial \rho_1}{\partial T} = -\frac{\partial v_{1z}}{\partial z}, \tag{16b}$$

which leads to linear wave equations for the particle velocity and density. In general, the frequencies of the waves are not resonant with a cavity eigenmode and the waves at any frequency are detuned, the detuning parameter being defined as

$$\delta_i = \omega_i^c - \omega_i, \tag{17}$$

where ω_i is the frequency of the field and ω_i^c is frequency of the cavity eigenmode closest to ω_i. In this case, the solution of the order $O(\varepsilon)$ takes the general form of a superposition of standing waves:

$$v_{1z} = \sum_{n=0}^{2} A_n(x,y,\tau)\sin[\omega_n T - (\phi_n(\tau) - \delta_i T)]\sin(k_n z), \tag{18}$$

where $\omega_n = k_n$. In Eq. (18) we have considered the frequency-selective effect of the walls discussed in the Introduction and assume that only three modes, those with frequencies obeying $\omega_1 + \omega_2 = \omega_0$, can reach significant amplitudes. Also, from Eqs. (16) we obtain that

$$\rho_1 = \sum_{n=0}^{2} A_n(x,y,\tau)\cos[\omega_n T - (\phi_n(\tau) - \delta_i T)]\cos(k_n z). \tag{19}$$

At order $O(\varepsilon^{3/2})$, the equations for the fast evolution of the transverse velocity components are obtained,

$$\frac{\partial v_{1x}}{\partial T} = -\frac{\partial \rho_1}{\partial x}, \tag{20a}$$

$$\frac{\partial v_{1y}}{\partial T} = -\frac{\partial \rho_1}{\partial y}. \tag{20b}$$

At order $O(\varepsilon^2)$ we get

$$\rho_1\frac{\partial v_{1z}}{\partial T} + \frac{\partial v_{2z}}{\partial T} + \frac{\partial v_{1z}}{\partial \tau} + \frac{1}{2}\frac{\partial^2 v_{1z}^2}{\partial z^2} + \frac{\bar{\Gamma}}{2}\frac{\partial \rho_1^2}{\partial z} - \bar{\mu}\frac{\partial^2 v_{1z}}{\partial z^2} + \frac{\partial \rho_2}{\partial z} = 0, \tag{21a}$$

$$\frac{\partial \rho_2}{\partial T} + \frac{\partial \rho_1}{\partial \tau} + \rho_1\frac{\partial v_{1z}}{\partial z} + \frac{\partial v_{2z}}{\partial z} + v_{1z}\frac{\partial \rho_1}{\partial z} + \frac{\partial v_{1x}}{\partial x} + \frac{\partial v_{1y}}{\partial y} = 0. \tag{21b}$$

Finally Eqs. (21), making use of the relations in Eqs. (20), can be reduced to a single wave equation for the density:

$$\frac{\partial^2 \rho_2}{\partial T^2} - \frac{\partial^2 \rho_2}{\partial z^2} = 2\frac{\partial^2 v_{1z}}{\partial z \partial \tau} - \bar{\mu}\frac{\partial^3 v_{1z}}{\partial z^3} + \frac{\bar{\Gamma}}{2}\frac{\partial^2 \rho_1^2}{\partial z^2} + \frac{\partial^2 v_{1z}^2}{\partial z^2} + \frac{\partial^2 \rho_1}{\partial x^2} + \frac{\partial^2 \rho_1}{\partial y^2}, \tag{22}$$

where the smaller-order solutions appear on the right-hand side as source terms.

A closed set of equations for the slowly varying envelopes of mode amplitudes A_n and phases ϕ_n can be obtained by substituting Eqs. (18) and (19) into Eq. (22) and imposing the absence of secular terms in the resulting equation—i.e., neglecting the source contributions that contain the same frequency components as the natural frequency of the left-hand-side part in Eq. (22). Otherwise, second-order solutions would grow linearly, violating the smallness condition $\varepsilon\rho_2 \ll \rho_1$ assumed in the perturbation expansion. After some algebra the secular terms reduce to the following real system for the amplitudes and phases:

$$\frac{\partial A_i}{\partial \tau} + \sigma s_i \omega_i A_j A_k \sin\phi + \frac{1}{2}\bar{\mu}\omega_i^2 A_i = 0, \tag{23a}$$

$$A_i\frac{\partial \phi_i}{\partial \tau} - \sigma\omega_i A_j A_k \cos\phi - \frac{1}{2\omega_i}\nabla_\perp^2 A_i - \delta_i A_i = 0, \tag{23b}$$

where $(i,j,k) = (0,1,2)$ and the other two equations are obtained by cyclic permutations. The sign operator $s_i = +1$ for $i = 1,2$ and -1 for $i = 0$. A global phase is defined as $\phi \equiv \phi_1 + \phi_2 - \phi_0$, $\nabla_\perp^2$ stands for the Laplacian operator acting on the transverse space $\mathbf{r}_\perp = (x,y)$, and σ is a coupling parameter defined as

$$\sigma = \frac{1}{4}\left(1 + \frac{B}{2A}\right). \tag{24}$$

Note that in Eqs. (23) the terms proportional to $\bar{\mu}$ account only for viscous losses. There are in fact other loss mechanisms, mainly related with finite reflectance of the walls or diffraction losses through the open sides of the resonator. When the losses are sufficiently small, one can generalize Eqs. (23) and consider an effective (phenomenological) loss parameter γ_i for each mode, just replacing $(\bar{\mu}/2)\omega_n^2 A_n$ by $\gamma_n A_n$. The value of these coefficents can be obtained experimentally for a particular resonator by small-amplitude measurements of the decay rate of a given mode, since under this condition (neglecting nonlinearity) the amplitudes obey $\partial A_n/\partial\tau = -\gamma_n A_n$.

Finally, for a dissipative resonator, an external source must be provided in order to compensate the losses. Consider that a plane wave of amplitude E and frequency ω_0^c is injected into the resonator. In each round-trip, the amplitude of the standing wave will increase by $2E$ and then

$$\frac{\Delta A_0}{\Delta t} = \frac{2E}{2L/c_0} = \frac{c_0}{L}E, \tag{25}$$

where L is the length of the resonator and c_0/L corresponds to the time taken for a wave to travel across it. By changing to the nondimensional notation in slow time scale and as-

suming small-amplitude changes during a round-trip, one can consider the differential limit of Eq. (25) and incorporate it into the evolution equation of A_0 as a driving term.

A particular case corresponds to the degenerate interaction, where $\omega_1=\omega_2$. This process describes subharmonic parametric generation. In this situation, the pump and subharmonic waves obey the relation $\omega_0=2\omega_1$. It is worth expressing the resulting system of equations in complex form by defining the complex amplitudes as $B_n(\mathbf{r}_\perp,\tau)=A_n(\mathbf{r}_\perp,\tau)\exp[i\phi_n(\tau)]$. At this point we also return to dimensional (physical) variables. Since amplitudes A_n correspond, e.g., to dimensionless densities and pressure is related to density by Eq. (5), then, in the degenerate limit, we obtain the following coupled equations for the evolutions of pressure:

$$\frac{\partial p_0}{\partial t}=-(\gamma_0+i\delta_0)p_0-i\frac{\sigma\omega_0}{\rho_0c_0^2}p_1^2+i\frac{c_0^2}{2\omega_0}\nabla_\perp^2p_0+\frac{c_0}{L}p_{in}, \tag{26a}$$

$$\frac{\partial p_1}{\partial t}=-(\gamma_1+i\delta_1)p_1-i\frac{\sigma\omega_1}{\rho_0c_0^2}p_1^*p_0+i\frac{c_0^2}{2\omega_1}\nabla_\perp^2p_1, \tag{26b}$$

together with their complex conjugate. In Eqs. (26), p_i corresponds to deviations from the equilibrium pressure values.

Equations (26) can be further simplified by adopting the normalizations

$$p_0=i\frac{2\rho_0c_0^2\gamma_1}{\sigma\omega_0}\mathcal{P}_0, \tag{27a}$$

$$p_1=\frac{\rho_0c_0^2\sqrt{2\gamma_0\gamma_1}}{\sigma\omega_0}\mathcal{P}_1, \tag{27b}$$

$$p_{in}=i\frac{2L\rho_0c_0\gamma_0\gamma_1}{\sigma\omega_0}\mathcal{E} \tag{27c}$$

and introducing the dimensionless detuning parameter $\Delta_n=\delta_n/\gamma_n$. The final form of the model reads

$$\frac{1}{\gamma_0}\frac{\partial\mathcal{P}_0}{\partial t}=-(1+i\Delta_0)\mathcal{P}_0-\mathcal{P}_1^2+ia_0\nabla_\perp^2\mathcal{P}_0+\mathcal{E}, \tag{28a}$$

$$\frac{1}{\gamma_1}\frac{\partial\mathcal{P}_1}{\partial t}=-(1+i\Delta_1)\mathcal{P}_1+\mathcal{P}_1^*\mathcal{P}_0+ia_1\nabla_\perp^2\mathcal{P}_1, \tag{28b}$$

where $a_n=c_0^2/2\omega_n\gamma_n$ are the diffraction coefficients. This form of the equations is relevant for our purposes, since their solutions and stability have been discussed in the context of nonlinear optics, after the model given by Eqs. (28) has been derived for the degenerate optical parametric oscillator. A detailed analysis of the spatiotemporal dynamics of Eqs. (28) has been carried out during the last decade (starting with the seminal work in [5]), and a recent overview can be found in [19]. In the following sections, we review the basic results regarding their homogeneous solutions and their stability, and we study numerically the spatiotemporal dynamics under conditions corresponding to a real acoustical resonator. Note that the connection between the generic model (28) and the particular acoustic problem is given by the normalizations performed in Eqs. (27).

III. MODULATIONAL INSTABILITIES OF HOMOGENEOUS SOLUTIONS

Two stationary states are solution of Eqs. (28): the simplest, trivial solution

$$\bar{\mathcal{P}}_0=\frac{\mathcal{E}}{(1+i\Delta_0)},\quad \bar{\mathcal{P}}_1=0, \tag{29}$$

characterized by a null value of the subharmonic field inside the resonator, and the nontrivial solution

$$|\bar{\mathcal{P}}_0|^2=1+\Delta_1^2, \tag{30a}$$

$$|\bar{\mathcal{P}}_1|^2=-1+\Delta_0\Delta_1\pm\sqrt{|\mathcal{E}|^2-(\Delta_0+\Delta_1)^2}, \tag{30b}$$

in which both the pump and the subharmonic fields have a nonzero amplitude and exist above a given (threshold) pump value $\mathcal{E}=\mathcal{E}_{th}$. At this value, given by

$$|\mathcal{E}_{th}|=\sqrt{(1+\Delta_0^2)(1+\Delta_1^2)}, \tag{31}$$

the trivial solution loses its stability and bifurcates into the nontrivial one. The emergence of this finite-amplitude solution corresponds to the process of subharmonic generation. Note that the fundamental amplitude above the threshold is independent of the value of the injected pump, which means that all the energy is transferred to the subharmonic wave.

These results have been confirmed experimentally for an acoustical resonator in [10]. The character of the bifurcation depends on the detuning values. As demonstrated in [10] and also in the optical context [18], the bifurcation is supercritical when $\Delta_0\Delta_1<1$ and subcritical when $\Delta_0\Delta_1>1$. In the latter case, both trivial and finite-amplitude solutions can coexist for given sets of the parameters, which results in a regime of bistability between different solutions.

In order to study the stability of the trivial solution (29) against space-dependent perturbations, consider a deviation of this state, given by $A_j(\mathbf{r}_\perp,t)=\bar{A}_j+\delta A_j(\mathbf{r}_\perp,t)$. Assuming that the deviations are small with respect to the stationary values, one can substitute the perturbed solution in Eqs. (28) and linearize the resulting system in the perturbations δA_j. The generic solutions of the linear system are of the form

$$(\delta A_j,\delta A_j^*)\propto e^{\lambda(k_\perp)t}e^{i\mathbf{k}_\perp\cdot\mathbf{r}_\perp}, \tag{32}$$

where $\lambda(\mathbf{k}_\perp)$ represents the growth rate of the perturbations and $\mathbf{k}_\perp$ is the transverse component of the wave vector, which in a two-dimensional geometry obeys the relation $|\mathbf{k}_\perp|^2=k_x^2+k_y^2$. The growth rates, which depend on the wave number of the perturbations, are obtained as the eigenvalues of the linear system. This analysis has been performed before [5], and we present here the main conclusions, omitting details.

The eigenvalue (and consequently the instabilities) presents a different character depending on the sign of the sub-

harmonic detuning. If $\Delta_1 > 0$, which corresponds to a subharmonic frequency smaller than that of the closest cavity mode, the eigenvalue shows a maximum at $k_\perp = 0$, the emerging solution being homogeneous in transverse space, with amplitude given by Eq. (30). On the contrary, in the opposite case $\Delta_1 < 0$, which corresponds to field frequencies larger than the nearest cavity mode, the maximum of the eigenvalue occurs for perturbations with transverse wave number

$$k_\perp = \sqrt{-\frac{\Delta_1}{a_1}}. \tag{33}$$

The emerging solution in this case is of the form of Eq. (32), which represents a plane wave tilted with respect to the cavity axis. This solution shows spatial variations in the transverse plane, and consequently pattern formation is expected to occur.

Since $k_\perp$ is the modulus of the wave vector, the linear stability analysis in two dimensions predicts that a continuum of modes within a circular annulus [centered on a critical circle at $|\mathbf{k}_\perp| = k_\perp$ in (k_x, k_y) space] grows simultaneously as the pump increases above a critical value. This double-infinite degeneracy of spatial modes (degenerate along a radial line from the origin and orientational degeneracy) allows, in principle, arbitrary structures in two dimensions.

The threshold for pattern formation follows also from the eigenvalue and is given by

$$\mathcal{E}_p = \sqrt{1 + \Delta_0^2}. \tag{34}$$

The predictions of the stability analysis correspond to the linear stage of the evolution, where the subharmonic field amplitude is small enough to be considered a perturbation of the trivial state. The analytical study of the further evolution would require a nonlinear stability analysis, not given here. Instead, in the next section we perform the numerical integration of Eqs. (28), where predictions of the acoustic subharmonic field in the linear and nonlinear regime are given.

IV. NUMERICAL RESULTS IN THE ACOUSTICAL CASE

The analytical predictions of the linear stability analysis have been numerically confirmed for Eqs. (28) in previous studies in the context of nonlinear optics. In this section we demonstrate the adequacy of these result for the acoustical case. For this aim, we first evaluate the different parameters appearing in Eqs. (26) for a concrete case.

Consider a resonator composed by two identical walls of thickness $D = H = 0.5$ cm made of a lead zirconate titanate (PZT) piezoelectric material ($c_t = 4400$ m/s, $\rho_t = 7700$ kg/m^3), containing water ($c_m = 1480$ m/s, $\rho_t = 1000$ kg/m^3). For this case $\mathcal{R} = 22.89$. The length of the medium L can be varied in order to modify detunings. If the resonator is driven at a frequency $f_0 = 4$ MHz, then subharmonic generation is expected to occur at $f_1 = 2$ MHz. The corresponding detunings have been numerically evaluated from Eq. (2). For a cavity length $L = 3$ cm, the pump is almost resonant with a cavity mode, $\delta f_0 = f_0^c - f_0 \approx 0$ kHz, and the subharmonic is detuned by $\delta f_1 = f_1^c - f_1 \approx -1.6$ kHz. Furthermore, under these conditions the second harmonic at $f_2 = 8$ MHz is highly detuned by $\delta f_2 = f_2^c - f_2 \approx -3.7$ kHz, and therefore it will reach a small amplitude.

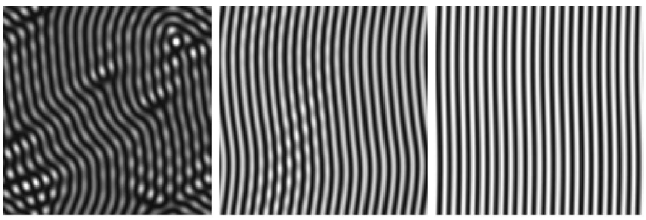

FIG. 2. Developement of stripped patterns for $\Delta_1 = -1.6$, $\Delta_0 = 0$, $\gamma_0 = \gamma_1 = 5 \times 10^3$, and $\mathcal{E} = 2$, as obtained by numerical integration of Eqs. (28). The distributions correspond to evolution times $t = 0.01$ s (a), $t = 0.1$ s (b), and $t = 1$ s (c).

The loss coefficients, as stated before, can be obtained for small-amplitude measurements of the decay rate of each mode in the resonator. In particular, a measurement of the quality factor for the different cavity modes, defined as $Q_i = \omega_i / 2\gamma_i$, was performed in [9] for a similar interferometer. For the frequencies of interest, the measured quality factors take values of the order of $10^3 - 10^4$. From this result we can conclude that reasonable values for the decay rates are $\gamma_0 = \gamma_1 = 5 \times 10^3$ rad/s, which allows us to evaluate the rest of the parameters in the model. The normalized detuning parameters corresponding to this case are $\Delta_0 = 0$ and $\Delta_1 = -1.6$, and diffraction coefficients result in $a_0 = 8.7 \times 10^{-6}$ and $a_1 = 2a_0$ Finally, the nonlinearity parameter of water at 20 °C is $B/A = 5$, which substituted in Eq. (24) gives $\sigma = 0.875$.

The theory of the previous section predicts that, when the threshold value Eq. (34) is achieved, a periodic pattern with a characteristic scale given by Eq. (33) develops. For the above conditions, the normalized threshold value is $\mathcal{E}_p = 1$, and the corresponding input pressure at the driving wall is obtained from the last of Eqs. (27) and results in $p_{in} \approx 0.1$ MPa. Also, the wavelength of the pattern is obtained from $\lambda_\perp = 2\pi / k_\perp \approx 1.5$ cm. Then, in order to observe the pattern the transverse section must contain several wavelengths, which in turn implies a transverse size of 10 cm or more. All these values can be considered as realistic.

In order to check the analytical predictions, we integrated numerically Eqs. (28) by using the split-step technique on a spatial grid of dimensions 128×128 [6]. The local terms, either linear (pump, losses and detuning) and nonlinear, are calculated in the space domain, while nonlocal terms (diffractions) are evaluated in the spatial wave-vector (spectral) domain. A fast Fourier transform (FFT) is used to shift from spatial to spectral domains in every time step. Periodic boundary conditions are used.

As initial condition, a noisy spatial distribution is considered and the parameters are those discussed above, for which a pattern forming instability is predicted. Figure 2 shows the result of the numerical integration. In Figs. 2(a) and 2(b) several snapshots of the evolution at different times are shown, which eventually result in a final stable one-

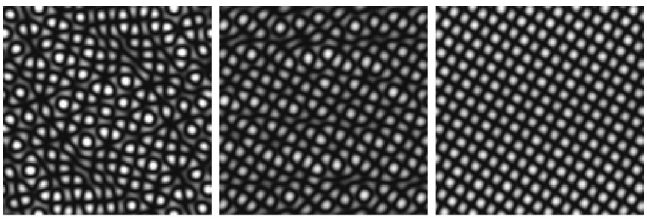

FIG. 3. Developement of squared patterns for $\Delta_1=-4$, $\Delta_0=-8$, $\gamma_0=\gamma_1=5\times10^3$, and $\mathcal{E}=1.2$, as obtained by numerical integration of Eqs. (28). The distributions correspond to evolution times $t=0.01$ s (a), $t=0.1$ s (b), and $t=1$ s (c).

dimensional pattern in the form of stripes, shown in Fig. 2(c).

Numerical simulations for different detunings have been performed. A systematic study shows that in most of the cases the system develops striped patterns with arbitrary orientations. However, in some cases a pattern with squared symmetry results as the final stable state. An example of evolution leading to squared patterns is shown in Fig. 3, obtained for $\Delta_1=-4$, $\Delta_0=-8$, and $\mathcal{E}=1.2$.

V. CONCLUSIONS

The pattern formation properties of an acoustical resonator where subharmonic generation takes place have been discussed from the theoretical point of view. A model allowing for diffraction of the fields (large-aspect-ratio limit) has been derived by means of the multiple-scale expansion technique. The obtained model, which turns out to be isomorphous to that obtained for optical parametric oscillator, has been analyzed in detail considering the distinctive peculiarities of the acoustical system. A typical acoustical configuration has been considered, and the predictions of the linear stability analysis have been confirmed by numerical integration of the model equations under realistic conditions. Numerics show that transverse patterns in the form of one-dimensional stripes are usually obtained as the final stable state, although the system can support also patterns with more complex structures, such as squares, hexagons, and localized structures.

The connection with optical parametric oscillation deserves one further comment: We would like to note that there has been several experimental attempts to verify the pattern formation scenario predicted by Eqs. (28) in a nonlinear optical resonator [20,21]. Although some transverse patterns with different latticelike structures have been observed, the use of other cavities different than planar (confocal and concentric) was required. Owing to the complete analogy between the model derived in this paper and the model describing optical parametric oscillation in planar resonators, we believe that the acoustical resonator could be a good candidate for the experimental observation of transverse patterns in a planar (Fabry-Perot) cavity. In such a way, the acoustical resonator could be helpful for checking an amount of theoretical predictions for optical parametric oscillation which presents an extremely hard experimental realization in optics.

Even more, as has been repeatedly shown [6,22], at certain limiting cases, optical parametric oscillation can be described by universal order parameter equations, such as the parametrically driven Ginzburg-Landau equation [22] in the large-pump-detuning limit or the real Swift-Hohenberg equation [6] in the small-pump-detuning case. The universal character of these ubiquitous order parameter equations establishes a tight connection of nonlinear acoustics not only with nonlinear optics, as mentioned aboved, but with the wider field of nonlinear science. We think that the recognition of these links could help to unify scattered research on pattern formation in nonlinear acoustics as well as help to observe phenomena difficult to observe in nonlinear systems different from acoustics. Experimental work in this direction is in progress.

ACKNOWLEDGMENTS

We thank E. Roldan for useful suggestions. The work has been financially supported by the CICYT of the Spanish Government, under Project No. BFM2002-04369-C04-04.

[1] M. C. Cross and P. C. Hohenberg, Rev. Mod. Phys. **65**, 851 (1993).
[2] J. W. Miles, J. Fluid Mech. **146**, 285 (1984).
[3] F. Melo, P. Umbanhowar, and H. L. Swinney, Phys. Rev. Lett. **72**, 172 (1994).
[4] V. L'vov, *Wave Turbulence Under Parametric Excitation* (Springer-Verlag, Berlin, 1994).
[5] G.-L. Oppo, M. Brambilla, and L. A. Lugiato, Phys. Rev. A **49**, 2028 (1994).
[6] G. J. de Valcárcel, K. Staliunas, E. Roldán, and V. J. Sánchez-Morcillo, Phys. Rev. A **54**, 1609 (1996).
[7] A. Korpel and R. Adler, Appl. Phys. Lett. **7**, 106 (1965).
[8] L. Adler and M. A. Breazeale, J. Acoust. Soc. Am. **48**, 1077 (1970).
[9] N. Yen, J. Acoust. Soc. Am. **57**, 1357 (1975).
[10] L. A. Ostrovsky and I. A. Soustova, Sov. Phys. Acoust. **22**, 416 (1976).
[11] D. Rinberg, V. Cherepanov, and V. Steinberg, Phys. Rev. Lett. **76**, 2105 (1996).
[12] F. V. Bunkin, Yu. A. Kravtsov, and G. A. Lyskhov, Sov. Phys. Usp. **29**, 607 (1986).
[13] M. F. Hamilton and J. A. TenCate, J. Acoust. Soc. Am. **81**, 1703 (1987).
[14] L. A. Ostrovsky, I. A. Soustova, and A. M. Sutin, Acustica **39**, 298 (1978).
[15] M. F. Hamilton and D. Blackstock, *Nonlinear Acoustics* (Academic Press, San Diego, 1998).
[16] L. K. Zarembo and O. Y. Serdoboloskaya, Akust. Zh. **20**, 726

(1974).
[17] N. S. Bakhvalov, Ya. M. Zhileikin, and E. A. Zabolotskaya, *Nonlinear Theory of Sound Beams* (American Institute of Physics, Woodbury, NY, 1997).
[18] L. A. Lugiato, C. Oldano, C. Fabre, E. Giacobino, and R. J. Horowicz, Nuovo Cimento D **10**, 959 (1988).
[19] K. Staliunas and V. J. Sánchez-Morcillo, *Transverse Patterns in Nonlinear Optical Resonators* (Springer, Berlin, 2003).
[20] S. Ducci, N. Treps, A. Maitre, and C. Fabre, Phys. Rev. A **64**, 023803 (2001).
[21] M. Vaupel, A. Maitre, and C. Fabre, Phys. Rev. Lett. **83**, 5278 (1999).
[22] S. Longhi, Phys. Scr. **56**, 611 (1997).